Articles

Structure and Function of the Xenobiotic Substrate Binding Site of a Glutathione *S*-Transferase As Revealed by X-ray Crystallographic Analysis of Product Complexes with the Diastereomers of 9-(*S*-Glutathionyl)-10-hydroxy-9,10-dihydrophenanthrene[†,‡]

Xinhua Ji,[§,∥] William W. Johnson,[§] Muctarr A. Sesay,[§] Laura Dickert,[§] Satya M. Prasad,[§] Herman L. Ammon,[§] Richard N. Armstrong,[*,§] and Gary L. Gilliland[*,∥,⊥]

Department of Chemistry and Biochemistry, University of Maryland, College Park, Maryland 20742, Center for Advanced Research in Biotechnology of the Maryland Biotechnology Institute, University of Maryland, Shady Grove, and of the National Institute of Standards and Technology, 9600 Gudelsky Drive, Rockville, Maryland 20850

Received September 9, 1993; Revised Manuscript Received November 8, 1993[⊕]

ABSTRACT: The three-dimensional structures of isoenzyme 3-3 of glutathione (GSH) transferase complexed with (9*R*,10*R*)- and (9*S*,10*S*)-9-(*S*-glutathionyl)-10-hydroxy-9,10-dihydrophenanthrene [(9*R*,10*R*)-**2** and (9*S*,10*S*)-**2**], which are the products of the addition of GSH to phenanthrene 9,10-oxide, have been determined at resolutions of 1.9 and 1.8 Å, respectively. The structures indicate that the xenobiotic substrate binding site is a hydrophobic cavity defined by the side chains of Y6, W7, V9, and L12 from domain I (the GSH binding domain) and I111, Y115, F208, and S209 in domain II of the protein. All of these residues are located in variable-sequence regions of the primary structure of class μ isoenzymes. Three of the eight residues (V9, I111, and S209) of isoenzyme 3-3 that are in direct van der Waals contact with the dihydrophenanthrenyl portion of the products are mutated (V9I, I111A, and S209A) in the related isoenzyme 4-4. These three residues are implicated in control of the stereoselectivity of the class μ isoenzymes. The hydroxyl group of Y115 is found to be hydrogen-bonded to the 10-hydroxyl group of (9*S*,10*S*)-**2**, a fact suggesting that this residue could act as an electrophile to stabilize the transition state for the addition of GSH to epoxides. The Y115F mutant isoenzyme 3-3 is about 100-fold less efficient than the native enzyme in catalyzing the addition of GSH to phenanthrene 9,10-oxide and about 50-fold less efficient in the Michael addition of GSH to 4-phenyl-3-buten-2-one. The side chain of Y115 is positioned so as to act as a general-acid catalytic group for two types of reactions that would benefit from electrophilic assistance. The results are consistent with the notion that domain II, which harbors most of the variability in primary structure, plays a crucial role in defining the substrate specificity of class μ isoenzymes.

The glutathione *S*-transferases (EC 2.5.1.18) catalyze the addition of the tripeptide glutathione (GSH) to xenobiotic substrates that have electrophilic functional groups. The catalytic diversity of this family of detoxification enzymes arises, in part, from the existence of numerous isoenzymes representing four distinct gene classes (Rushmore & Pickett, 1993). Although each isoenzyme generally exhibits a relatively broad substrate selectivity, most have unique catalytic attributes that are important in defining the role of a particular isoenzyme in the metabolism of endogenous and xenobiotic electrophiles (Armstrong, 1991, 1994). Considerable effort has been expended to document the substrate preferences of numerous isoenzymes from the various gene classes and species. Yet there is little information available concerning the precise enzyme—substrate interactions that may be responsible for the catalytic properties of any isoenzyme.

The recent determination of the three-dimensional structures of GSH transferases from the π, μ, and α classes (Reinemer *et al.*, 1991, 1992; Ji *et al.*, 1992; Sinning *et al.*, 1993) has offered the first glimpse of the xenobiotic substrate binding sites of this group of enzymes. Some general hypotheses have been advanced concerning the location and topology of this site based on the structures of the μ and π class enzymes complexed with GSH (Ji *et al.*, 1992) and the analogue glutathione sulfonate (Reinemer *et al.*, 1991), respectively. The structure of both dimeric proteins indicates that the subunits are composed of two domains, with the smaller N-terminal α/β domain (domain I) supplying all but one or two of the ionic contacts with the physiological substrate GSH. Although it is hard to escape the conclusion that domain I constitutes a GSH binding domain, it is less obvious whether the larger domain II (the C-terminal two-thirds of the protein) can be considered a "xenobiotic substrate" binding domain, as we have recently suggested (Ji *et al.*, 1992; Zhang *et al.*, 1992). The crystal structures of the π class isoenzyme from human placenta complexed with *S*-hexylglutathione at 2.8-Å resolution (Reinemer *et al.*, 1992) and the 2.6-Å resolution

[†] This work was supported by grants from the National Institutes of Health (GM30910) and the American Cancer Society (BC 632).

[‡] The final coordinates for the structures of the enzyme in complex with (9*S*,10*S*)- and (9*R*,10*R*)-9-(*S*-glutathionyl)-10-hydroxy-9,10-dihydrophenanthrene have been deposited in the Brookhaven Protein Data Bank under file names 2GST and 3GST, respectively.

* Address correspondence to these authors.

[§] University of Maryland at College Park.

[∥] Center for Advanced Research in Biotechnology of the Maryland Biotechnology Institute.

[⊥] National Institute of Standards and Technology.

[⊕] Abstract published in *Advance ACS Abstracts,* January 15, 1994.

0006-2960/94/0433-1043$04.50/0

Scheme 1

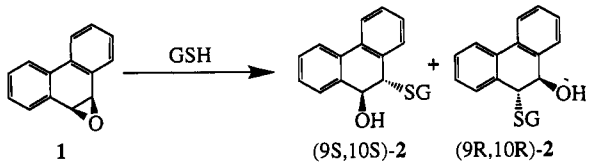

1 (9S,10S)-2 (9R,10R)-2

structure of the human α class isoenzyme complexed with *S*-benzylglutathione (Sinning *et al.*, 1993) show that residues from domain II help form the binding pocket for the organic substituents on sulfur.

Isoenzymes of the μ class GSH transferases share a high degree of sequence similarity (typically about 78% sequence identity), yet exhibit quite different catalytic characteristics. Analyses of the primary structures of the isoenzymes from rats (Abramovitz & Listowsky, 1987; Zhang & Armstrong, 1990; Zhang *et al.*, 1992) have revealed two important features of the sequence variability. One is the fact that the sequence differences are clustered in four variable regions. The second is that most of the sequence differences (three of the four variable regions) are located in the C-terminal two-thirds of the protein, domain II. The latter fact could be taken to suggest that domain II is either largely unnecessary with respect to the central catalytic function of the enzyme or that it evolved as a structurally malleable domain, which can be adjusted to provide isoenzymes with different specificities. The three-dimensional structure of the μ class isoenzyme 3-3 from rat indicates that three of the four variable regions (two of the three in domain II) are positioned close to and probably constitute part of the xenobiotic substrate binding site (Ji *et al.*, 1992). The structural details of the enzyme–substrate or enzyme–product interactions have not been elucidated.

The stereoselectivities of isoenzymes 3-3 and 4-4 from rat toward arene oxide substrates provide an interesting and well-documented example of a difference in catalytic characteristics between two closely related isoenzymes. The type 4 subunit is stereospecific in the addition of GSH to the oxirane carbon of *R* absolute configuration in phenanthrene 9,10-oxide (**1**) (Scheme 1), giving exclusively the (9*S*,10*S*) diastereomeric product, (9*S*,10*S*)-**2**. In contrast, the type 3 subunit is less efficient and exhibits little stereoselectivity in this reaction (Boehlert & Armstrong, 1984). Although the exact reasons for this difference in catalysis have not been determined, the construction and analysis of chimeric isoenzymes have provided functional evidence which suggests that the variable domains of the μ class isoenzymes contribute to the architecture of the active site (Zhang & Armstrong, 1990; Zhang *et al.*, 1992). Specifically, residues contained in variable region 1 at the N-terminus of domain I and in variable region 4 at the C-terminus of domain II have been implicated as affecting the stereoselectivity of the type 3 and 4 subunits. However, the identification or specific role of individual residues in these regions remains largely unknown.

In this article, we report the three-dimensional structures of the diastereomeric complexes of isoenzyme 3-3 of GSH transferase from rat with (9*S*,10*S*)- and (9*R*,10*R*)-9-(*S*-glutathionyl)-10-hydroxy-9,10-dihydrophenanthrene (**2**), the products of the reaction of GSH with phenanthrene 9,10-oxide. The two structures establish that the previous configurational assignments (Cobb *et al.*, 1983a) of the diastereomers are correct and reveal several specific interactions between the products and residues in variable regions 1, 2, and 4 that contribute to the observed catalytic characteristics of the type 3 and 4 subunits. Although the main chains of the two binary complexes are quite similar, a number of side-chain movements occur to accommodate the different diastereomers. The structures also implicate the hydroxyl group of Y115 as an electrophilic participant in the addition of GSH to epoxides and to α,β-unsaturated ketones. The role of Y115 in the catalytic mechanism is consistent with the kinetic properties of the Y115F mutant toward phenanthrene 9,10-oxide (Johnson *et al.*, 1993) and 4-phenyl-3-buten-2-one.

Table 1: Summary of Data Collection for Product Complexes

	(9*S*,10*S*)-**2**	(9*R*,10*R*)-**2**
D_{min} (Å)	1.8	1.9
total data observed	168 166	94 783
unique data observed	42 010	34 613
data with $I \geq 2\sigma(I)$	40 244	33 241
R_w[a]	8.83	8.37
R_{uw}[b]	7.32	6.49

[a] The weighted least-squares *R* factor on intensity for symmetry-related observations: $R_w = \sum[(Ii - G_{ij}\langle I\rangle j)/\sigma_{ij}]^2/\sum(I_{ij}/\sigma_{ij})^2$, where $G_{ij} = g_i + A_i s_j + B_i s_j^2$, $s = \sin\theta/\lambda$, and *g*, *A*, and *B* are scaling parameters. [b] The unweighted absolute *R* factor on intensities: $R_{uw} = \sum(I_{ij} - G_{ij}\langle I\rangle_j/\sum|I_{ij}|)$.

EXPERIMENTAL PROCEDURES

General Materials and Methods. Isoenzyme 3-3 of rat liver glutathione *S*-transferase was either purified from rat liver as previously described (Cobb *et al.*, 1983a) or expressed in and purified from *Escherichia coli* (M5219) harboring the expression plasmid pGT33MX (Zhang *et al.*, 1991). The Y115F mutant of isoenzyme 3-3 was prepared as described by Johnson *et al.* (1993). The (9*R*,10*R*) and (9*S*,10*S*) diastereomers of 9-(*S*-glutathionyl)-10-hydroxy-9,10-dihydrophenanthrene were synthesized and separated as previously described (Chung *et al.*, 1987). Assay of the enzymes with 4-phenyl-3-buten-2-one was carried out at pH 6.5, as described by Zhang *et al.* (1992). Crystals of isoenzyme 3-3 in complex with (9*R*,10*R*)-**2** were obtained as described by Sesay *et al.* (1987) either with enzyme isolated from rat liver or with the recombinant protein. The recombinant protein was used to obtain crystals with (9*S*,10*S*)-**2** in a manner identical to that described by Ji *et al.* (1992), except that this diastereomer was substituted for (9*R*,10*R*)-**2**. X-ray diffraction data were collected from single crystals of the two product complexes using a Siemens electronic area detector and a Rigaku rotating anode X-ray source, as previously described (Ji *et al.*, 1992).[1] The raw data frames were processed on a Silicon Graphics Personal IRIS computer using the XENGEN suite of programs (Howard *et al.*, 1987). The data sets for the complexes with (9*S*,10*S*)-**2** and (9*R*,10*R*)-**2** were 96% complete to 1.80 Å and 92.7% complete to 1.90 Å, respectively. The average $I/\sigma(I)$ was >3 for the highest resolution shells in both data sets. Data collection statistics are summarized in Table 1 with more details given in Table II of the supplementary material.

Crystallographic Refinement. The starting model for the refinement of the enzyme–(9*R*,10*R*)-**2** complex was the 2.2-Å resolution model of isoenzyme 3-3 complexed with glutathione (Ji *et al.*, 1992), after the deletion of both GSH molecules and all 474 water molecules. The model of the enzyme complexed with (9*R*,10*R*)-**2** was, in turn, used as the starting model for the refinement of the (9*S*,10*S*)-**2** complex. The refinement

[1] Certain commercial equipment, instruments, and materials are identified in this paper in order to specify the experimental procedure as completely as possible. In no case does such identification imply a recommendation or endorsement by the National Institute of Standards and Technology, nor does it imply that the material, instrument, or equipment identified is the best available for the purpose.

Table 2: Summary of Least-Squares Refinement Parameters for Product Complexes

	product	
	(9*S*,10*S*)-**2**	(9*R*,10*R*)-**2**
resolution range (Å)[a]	6.0–1.8	6.0–1.9
reflections measured	39 002	32 042
reflections used with $I \geq 2\sigma(I)$	35 708	28 714
crystallographic *R* factor[b]	0.160	0.159
number of		
residues	434	434
water molecules	470	437
sulfate ions	2	7
non-H protein atoms/water molecules	7.7	8.3
rms deviations from ideal distances (Å)		
bond distances	0.020	0.019
bond angles	0.035	0.030
planar 1–4 distances	0.041	0.034
rms deviations from ideal chirality (Å^3)	0.229	0.200
thermal parameter correlation (mean/$\Delta\beta$)		
main-chain bond	0.797	0.742
main-chain angle	1.249	1.208
side-chain bond	1.683	1.408
side-chain angle	2.470	2.140

[a] Data used for least-squares refinement. All data were used in the calculation of electron density maps. [b] Crystallographic $R = \sum_{hkl}||F_o| - |F_c||/\sum_{hkl}|F_o|$.

was performed on a CRAY Y-MP computer with GPRLSA (Furey *et al.*, 1982), the restrained least-squares refinement procedure of Hendrickson and Konnert (1980a,b) and Hendrickson (1985a,b). FRODO (Jones, 1978) was used on an Evans & Sutherland PS390 graphics system supported by a MicroVAXII computer for the examination of $2F_o - F_c$, $F_o - F_c$, and omit maps, the adjustment of the model, and the deletion and addition of water molecules.

The entire model was checked and adjusted when necessary. Water molecules and sulfate anions were located in the difference electron density maps as peaks higher than 3σ. After all of the possible solvent molecules were found, they were verified by a series of omit maps (Furey, 1990) with 100 water molecules deleted each time. This procedure was performed in ascending order starting from the bottom of the list of water molecules ranked according to the parameter OCC^2/B (James & Sielecki, 1983), the ratio of the square of the fractional occupancy factor (OCC) of the oxygen atom position and the crystallographic temperature factor (*B*). Lower resolution diffraction data excluded from the refinement were included in all map calculations. A summary of the crystallographic refinement is found in Table 2. The final coordinates for both structures have been deposited in the Brookhaven Protein Data Bank (Bernstein *et al.*, 1977) under file names 2GST and 3GST.

RESULTS

Crystal Structure and Absolute Configuration of Product Complexes. Figures 1 and 2 illustrate the initial $F_o - F_c$ and final $2F_o - F_c$ electron density maps for the two diastereomers of **2** complexed with isoenzyme 3-3. Modeling of the products posed no particular problems in the refinement. In principle, the 9,10-dihydrophenanthrenyl ring system with trans-configured substituents can exist in two conformations, with the hydroxyl and glutathionyl substituents occupying either the pseudo-diaxial or pseudo-diequatorial positions. The initial model of each diastereomer was constructed on the basis of the fact that the favored conformation both in aqueous solution (Cobb *et al.*, 1983a,b) and bound to the enzyme (Chen *et al.*, 1986) is the one with diaxial substituents. Single orientations of the product models eliminated virtually all of the difference electron density in the active-site cavity (Figures 1a and 2a), suggesting that the dihydrophenanthrenyl portion of the products is bound in essentially a single orientation of one conformation.

The configurational assignments of the two diastereomeric products were originally based on the chiroptical properties of the twisted biphenyl chromophore and the pseudo-diaxial orientation of the glutathionyl and hydroxyl substituents as determined by NMR spectroscopy (Cobb *et al.*, 1983a,b). It was, therefore, important to ascertain whether the absolute configurations of the two products were assigned correctly and were consistent with the difference electron density maps. The initial $F_o - F_c$ map of enzyme complexed with (9*R*,10*R*)-**2** was calculated without refinement by using the coordinates of the 434 residues of the 2.2-Å resolution structure (Ji *et al.*, 1992). Similarly, refined 1.9-Å resolution coordinates of the (9*R*,10*R*)-**2** product complex (this work) were used to calculate the initial structure factors of the (9*S*,10*S*)-**2** complex before the crystallographic refinement was carried out. As shown in Figures 1a and 2a, the complete $F_o - F_c$ map of each product complex fits only the appropriate diastereomer, suggesting that the original assignments of configuration are correct. Moreover, the helicity of the biphenyl ring system and the diaxial disposition ofglutathionyl and hydroxyl substituents are readily apparent from both the initial $F_o - F_c$ (Figures 1a and 2a) and the final $2F_o - F_c$ maps (Figures 1b and 2b). Also illustrated in Figures 1b and 2b is the conformational difference of the γ-Glu residue in the product complexes. This is due to the nonbonded steric interaction between OE, the carbonyl oxygen atom of γ-Glu peptide bond, and the carbinol carbon of (9*R*,10*R*)-**2**.

Several years ago, some preliminary evidence was presented that suggested that GSH transferases might be posttranslationally methylated (Siegel *et al.*, 1990). More specifically, the μ class subunit types 3 and 4 were reported to be substrates for a calmodulin-stimulated GSH transferase, methyltransferase. The availability of crystals of isoenzyme 3-3 isolated from rat liver complexed with (9*R*,10*R*)-**2** allowed us to address this question crystallographically. A careful examination of protein side chains likely to be methylated (e.g., lysine and arginine) showed no unexplained electron density that might be associated with the presence of a methyl group. Thus, if methylation of isoenzyme 3-3 occurs, it must be sufficiently rare so as to be crystallographically transparent.

Protein–Product Interactions. The structures of isoenzyme 3-3 complexed with (9*S*,10*S*)-**2** and (9*R*,10*R*)-**2** are quite similar, except in the immediate vicinity of the active site. The root-mean-square (RMS) difference for all 434 α-carbon atoms between the product complexes is 0.13 Å, while it is about 0.21 Å when either product complex is compared with the enzyme–GSH complex (Ji *et al.*, 1992). Interactions between the protein and the glutathionyl portion of both products are basically identical to those seen in the structure of the enzyme in complex with GSH (Ji *et al.*, 1992). The 1.8-Å structure of the complex with (9*S*,10*S*)-**2** reveals several van der Waals contacts between the dihydrophenanthrenyl ring system and side chains in the active site, including those of Y6, W7, V9, and L12 in domain I and I111, Y115, F208, and S209 in domain II, as illustrated in Figure 3. The ring system occupies a hydrophobic pocket defined by the side chains of V9 and L12 on one side and I111, Y115, F208, and S209 on the other. In addition, the hydroxyl group of Y115 of subunit A forms a hydrogen bond (3.3 Å, Figure 3a) with the 10-hydroxyl group of the (9*S*,10*S*) product, but is somewhat farther away (3.8 Å) in subunit B. This particular difference between subunits A and B appears to be the result

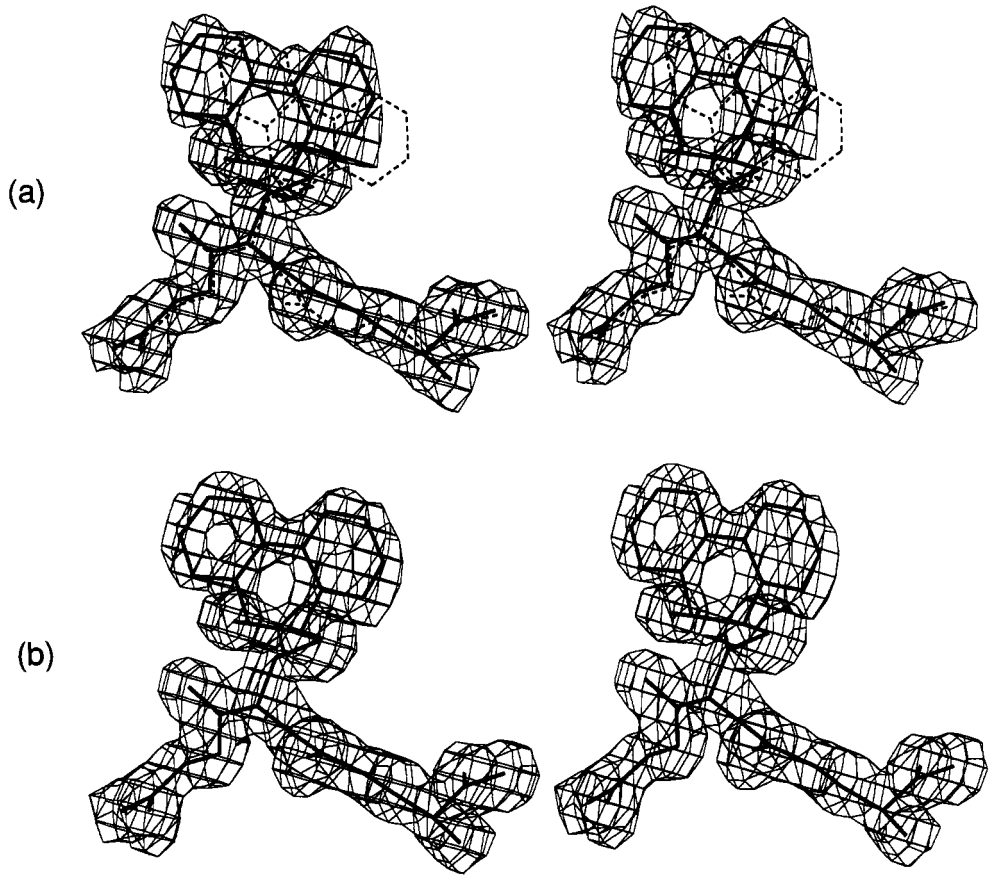

FIGURE 1: Stereoviews of (a) the initial $F_o - F_c$ map contoured at 2σ and (b) the final $2F_o - F_c$ map contoured at 1σ for glutathione *S*-transferase 3-3 (subunit A) complexed with (9*S*,10*S*)-9-(*S*-glutathionyl)-10-hydroxy-9,10-dihydrophenanthrene. Average *B* factors for the glutathionyl and dihydrophenanthrenyl portions of the product are 12.0 and 17.1 Å^2, respectively. The structure represented by the solid line is of the final model, and that in the dashed line illustrates the other diastereomer.

of differences in the crystal packing contacts of the two subunits with neighboring molecules.

The dihydrophenanthrenyl ring system of (9*R*,10*R*)-**2** occupies essentially the same plane as the (9*S*,10*S*) diastereomer, but is shifted by about 1.5 Å (Figure 3c). Most of the side-chain interactions with the dihydrophenanthrenyl moiety are preserved in the structure of the complex with the (9*R*,10*R*) diastereomer. Although the main chains in the two diastereomeric product complexes are essentially identical in structure, there are significant movements of several side chains that make contact with the dihydrophenanthrenyl ring system, as illustrated in Figure 3c. It is interesting to note that, even though the dihydrophenanthrenyl group makes several contacts with side chains in domain I (e.g., Y6, W7, V9, and L12), the positions of these side chains are essentially unchanged (<0.5 Å in both subunits) from those in the complex with (9*S*,10*S*)-**2** (Figure 3c). Significant side-chain movements are confined to residues located in domain II. In particular, CD of I111 is displaced by 2.8 Å (2.7 Å in subunit B) to avoid unfavorable contact with the dihydrophenanthrenyl moiety. Furthermore, the hydroxyl group of Y115 moves about 0.9 Å (also in subunit B) and out of hydrogen-bonding distance of the 10-hydroxyl group of (9*R*,10*R*)-**2**. The movement of Y115 plus the 1.7-Å (1.5 Å in subunit B) change in the position of the 10-hydroxyl group places these two groups 5.5 Å (5.6 Å in subunit B) apart, where they hydrogen bond to the same water molecule (Figure 3b,c).

Electrophilic Catalysis by Y115. The close proximity of the hydroxyl group of Y115 to the 10-hydroxyl group of the (9*S*,10*S*) product suggests that Y115 might be located close enough to the oxirane oxygen in the transition state for epoxide ring opening to provide some electrophilic assistance in this reaction either directly or through an intervening water molecule. This possibility was suggested recently by the finding that the Y115F mutant is about 10^2-fold less efficient than the native enzyme in the addition of GSH to **1** (Johnson *et al.*, 1993). A similar result is found here in the enzyme-catalyzed addition of GSH to 4-phenyl-3-buten-2-one (Table 3), another reaction that would benefit from electrophilic assistance. In neither case is the decrease in the efficiency of the mutant accompanied by a significant change in stereoselectivity. The electrophilic assistance is, therefore, manifest almost equally in both diastereomeric transition states. These observations tend to suggest that the hydroxyl group of Y115 may serve as a general-acid catalytic group in a wide range of reactions catalyzed by GSH transferases.

Solvent Structure. A total of 470 water molecules is observed in the crystal structure of isoenzyme 3-3 complexed with (9*S*,10*S*)-**2**; of these, 386 form hydrogen bonds to the protein. By comparison, 340 out of 437 water molecules observed in the enzyme–(9*R*,10*R*)-**2** (E·(9*R*,10*R*)-**2**) structure are hydrogen-bonded to the enzyme. Each water molecule included in the final model of the two structures is hydrogen-bonded to other atom(s). More than one-half (254) of the water molecules can be located in either of these two structures or in the structure of the enzyme–GSH (E·GSH) complex (Ji *et al.*, 1992) and can be considered an integral part of the crystal structure. Sixteen water molecules included in the original 2.2-Å resolution structure (Ji *et al.*, 1992) did not appear to be hydrogen-bonded to any other atom. Eleven of these are found, in the higher resolution structures examined

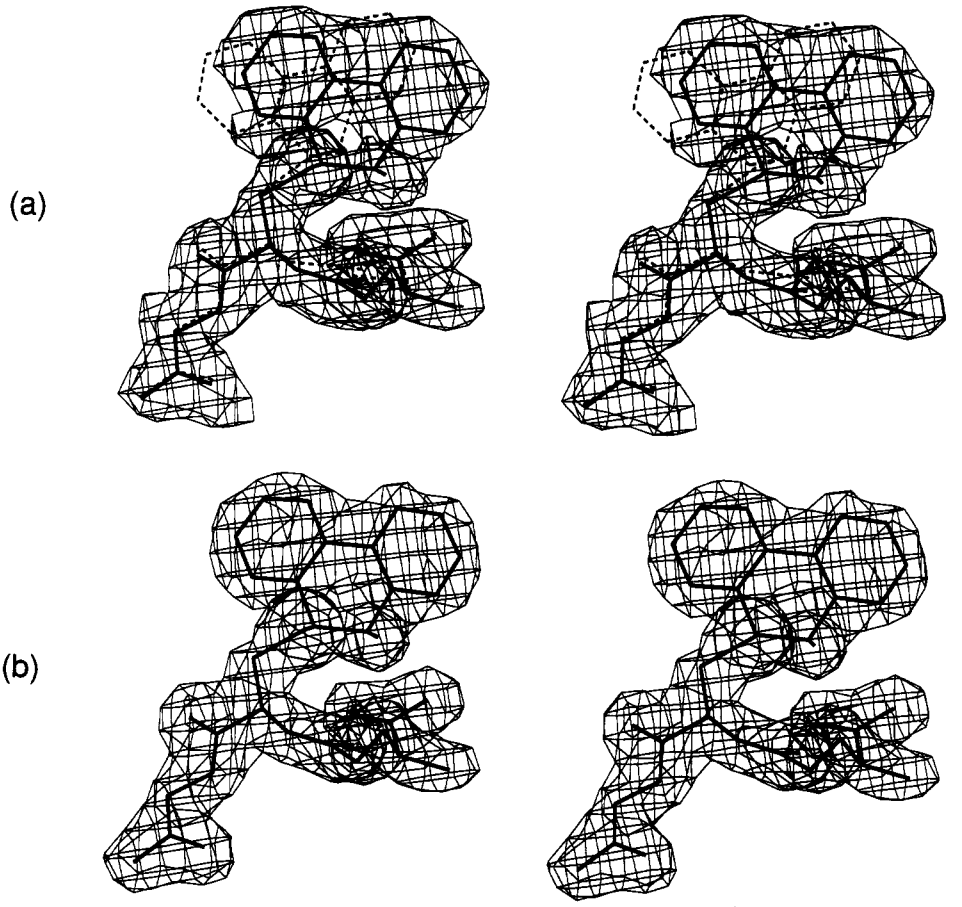

FIGURE 2: Stereoviews of (a) the initial $F_o - F_c$ map contoured at 2σ and (b) the final $2F_o - F_c$ map contoured at 1σ for glutathione *S*-transferase 3-3 (subunit A) complexed with (9*R*,10*R*)-9-(*S*-glutathionyl)-10-hydroxy-9,10-dihydrophenanthrene. Average *B* factors for the glutathionyl and dihydrophenanthrenyl portions of the product are 15.6 and 19.2 Å^2, respectively. The structure represented by the solid line is of the final model, and that in the dashed line illustrates the other diastereomer.

in this work, to form hydrogen bonds to nearby water molecules.

One water molecule of particular interest is located in the active site and is conserved in all of the structures of isoenzyme 3-3 that have been determined. The water is within hydrogen-bonding distance of O(G11), NH1(R107), OE1(Q165), and NE2(Q165) and appears to be an integral part of the active site. For example, it is within van der Waals contact distance with the dihydrophenanthrenyl groups of the products and may constitute a repulsive contact that is significant in catalysis.

Two sulfate anions are included in the final model of the enzyme complexed with (9*S*,10*S*)-**2** and seven in the E·(9*R*,10*R*)-**2** complex. All but one of the sulfates are hydrogen-bonded to the nitrogen atom of a positively charged side chain. The one that is not hydrogen-bonded to a cationic group is, however, conserved in both structures. It resides at one end of the solvent channel close to the active site of subunit B. There are two possible factors that may stabilize this sulfate anion. First, it is close to the α-amino group of the tripeptide product. The distance from the α-NH_4^+ of the γ-glutamyl residue to the closest oxygen atom of this sulfate anion is 4.6 Å in E·(9*S*,10*S*)-**2** and 5.0 Å in the other. Secondly, the α-carboxylate of the γ-glutamyl group of the product is on the axis of and within 4 Å of the N-terminal end of the α3-helix (Ji *et al.*, 1992). Therefore, the α3-helix dipole (positive), the α-carboxylate of the γ-glutamyl group (negative), the α-amino group of the tripeptide (positive), and the sulfate anion (negative) form a favorable alternating charge interaction pattern, which may significantly stabilize this sulfate anion. At lower contour levels (0.75σ $2F_o - F_c$ map or 2σ $F_o - F_c$ map), extra electron density can be seen at about the same positions in subunit A of both structures, which may reasonably be considered sulfate anions with low occupancy factors. This is also true for nonconserved sulfates in the two structures.

Relative Mobility and Ligand Exchange Behavior of the Two Subunits. The locations of crystal contacts in the primary structures of subunits A and B, which are illustrated in Figure 4, are basically the same as those found in the crystal structure of GSH transferase complexed with GSH (Ji *et al.*, 1992). The apparent segmental motion of the two subunits as represented by the residue-averaged thermal parameters for main-chain atoms of the enzyme complexed with (9*S*,10*S*)-**2** and (9*R*,10*R*)-**2** is illustrated in Figure 4. As previously reported, one of the consequences of the intermolecular interactions of crystal packing is that domains IA and IIB have fewer contacts with symmetry-related molecules than IB and IIA and, therefore, are more mobile than the latter pair. Careful examination of Figure 4 shows this to be the case for the two product complexes as well.

Three regions of the polypeptide that are near the active site exhibit higher than average thermal parameters (Figure 4). Together these three regions, residues 33–43 (the μ loop), 110–130 (the C-terminal half of the α4-helix and α5a, which are connected by a tight two-residue turn), and 205–217 (the C-terminal tail), constitute structural elements that help define a channel to the active site. One face of the C-terminal half of the α4-helix and parts of the C-terminal tail form two walls of the active site. The thermal parameters for these three

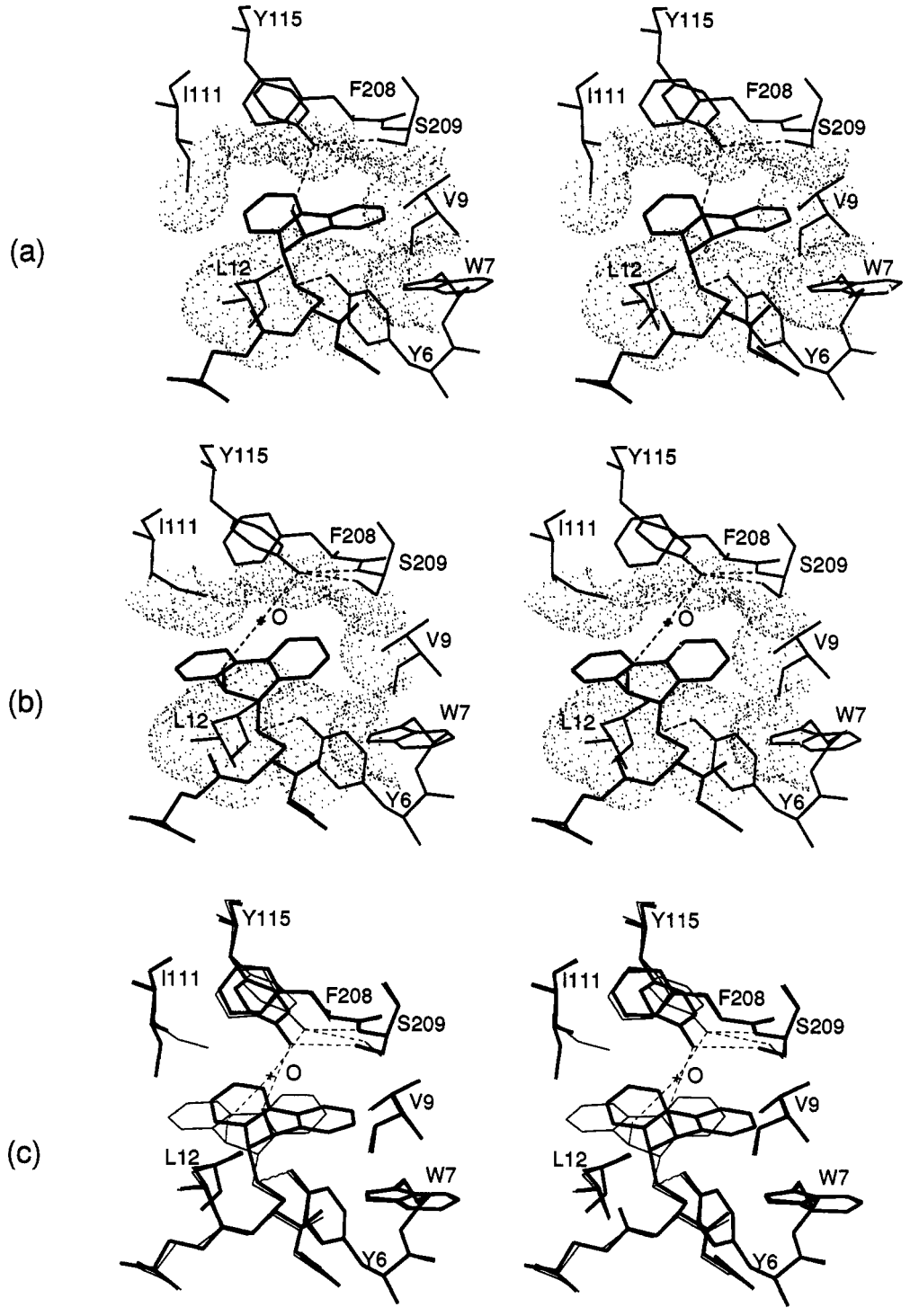

FIGURE 3: Stereoviews of the xenobiotic substrate binding site in subunit A of glutathione *S*-transferase 3-3 complexed with (9*S*,10*S*)-9-(*S*-glutathionyl)-10-hydroxy-9,10-dihydrophenanthrene (a) and (9*R*,10*R*)-9-(*S*-glutathionyl)-10-hydroxy-9,10-dihydrophenanthrene (b). The shape of the hydrophobic pocket is illustrated in the dotted surfaces. The two diastereomeric structures are compared in c, showing the different hydrogen-bonding patterns and the movements of the side chains of I111, Y115, F208, and S209.

Table 3: Kinetic Constants and Stereoselectivity for the Addition of GSH to 4-Phenyl-3-buten-2-one Catalyzed by Isoenzyme 3-3 and the Y115F Mutant

enzyme	k_{cat} (s^{-1})	k_{cat}/K_m (M^{-1} s^{-1})	% isomer A
native	0.38 ± 0.04	(2.68 ± 0.04) × 10^3	50 ± 3
Y115F	0.020 ± 0.003	(7.47 ± 0.30) × 10^1	41 ± 2

regions in subunit A of both structures are generally lower than those in subunit B (Figure 4), a fact that appears to correlate with the extent of hydrogen-bonding interactions between the three structural elements, as summarized in Table 4. The extent of hydrogen-bonding interactions clearly depends on what ligand occupies the active site. Only two of the five interactions are conserved in both subunits of all three structures. The ramifications of the hydrogen-bonding networks and subunit mobility on product release rates are discussed below.

We previously reported that replacement of the product inhibitor in crystals of the E·(9*R*,10*R*)-**2** complex with either GSH or *S*-(3-iodobenzyl)glutathione is readily accomplished by diffusion at 25 °C in 4–6 h (Ji *et al.*, 1992). The exchange is complete in both subunits. In contrast, similar experiments

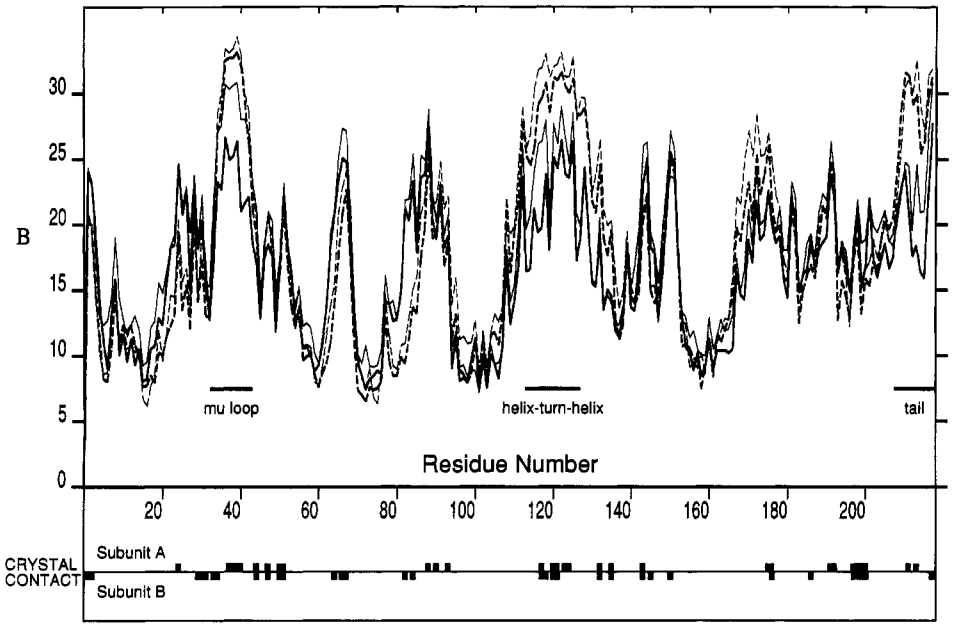

FIGURE 4: Plots of the residue-averaged thermal factors (B) as a function of main-chain atoms for the two subunits of the final models for the product structures. The traces for subunits A and B are shown as solid and broken lines, respectively. The traces for E·(9*S*,10*S*)-**2** and E·(9*R*,10*R*)-**2** are distinguished by the bold and light lines, respectively. The thermal parameters for the two structures were not scaled. Average B factors (main chain, side chain) for E·(9*S*,10*S*)-**2** and E·(9*R*,10*R*)-**2** are (15.7, 17.3 Å^2) and (17.3, 18.5 Å^2), respectively. The regions of sequence involved in crystal contacts are illustrated by the bold bars at the bottom.

Table 4: Intramolecular Hydrogen Bonds Found between the μ Loop (Residues 33–43), the α4/α5-Helix–Turn–Helix (Residues 100–130), and the C-Terminal Tail (Residues 205–217) in the Crystal Structures of Isoenzyme 3-3 Complexed with (9*S*,10*S*)-**2**, (9*R*,10*R*)-**2** (This Work), and GSH (Ji *et al.*, 1992)

intramolecular hydrogen bonds	hydrogen-bond distances (Å[a]) for subunits A and B					
	(9*S*,10*S*)-**2**		(9*R*,10*R*)-**2**		GSH	
	A	B	A	B	A	B
(Met34)O···(Lys210)NZ	2.8		3.0	3.4		
(Asp36)OD1···(Lys210)NZ	2.3		2.8			
(Cys114)O···(Gln213)N	2.6	2.9	2.9	2.9	2.7	2.9
(Tyr115)OH···(Ser209)N			3.3	3.3	3.2	3.5
(Tyr115)OH···(Ser209)OG	2.9	3.3	2.8	2.6	2.8	2.5

[a] The hydrogen-bond distance cutoff was set at 3.5 Å.

with the crystalline E·(9*S*,10*S*)-**2** complex indicate that complete exchange of this product with other ligands such as GSH is much more difficult. Although complete replacement of (9*S*,10*S*)-**2** with GSH in subunit B can be accomplished by soaking the crystals in excess GSH for several days, no exchange is observed in subunit A. This fact appears to correlate with the lower thermal factors seen in subunit A for the three elements that define the approach to the active site. The direct hydrogen-bonding interaction between the hydroxyl group of Y115 and the hydroxyl group at the 10-position of (9*S*,10*S*)-**2** may also contribute to the lower exchange rate in the crystal.

DISCUSSION

Structure of the Xenobiotic Substrate Binding Site. Previous studies have offered a glimpse of the regions of polypeptide or residues that might be involved in the architecture of the xenobiotic substrate binding site of μ class GSH transferases. Comparisons of the primary structures of μ class GSH transferases from rat have led to the conclusion that sequence variations in the polypeptide are grouped in four so-called variable regions (Abramovitz & Listowsky, 1987; Zhang & Armstrong, 1990). Figure 5 illustrates the relationship between the variable-sequence regions, the secondary structural elements, and the domain structure of isoenzyme 3-3. It is striking that all eight of the residues that make direct van der Waals contacts with the xenobiotic portion of the product reside in variable regions of the μ class sequences. Three of the eight residues (denoted with asterisks) differ in the sequences of the type 3 and 4 subunits. Thus, the type 4 subunit, which has a much higher efficiency and stereoselectivity toward arene oxide and α,β-unsaturated ketone substrates, has mutations (V9I, I111A, and S209A) in residues that directly contact the xenobiotic portion of the products in the type 3 subunit. It is likely that the variable regions of the μ class isoenzymes, which are primarily, though not exclusively, located in domain II of the protein, have evolved as a mechanism to increase the catalytic diversity of the GSH transferases. Although several residues in domain I also contribute to the structure of the xenobiotic substrate binding site by virtue of their proximity to the sulfur of bound GSH, the main function of the domain I is to bind the tripeptide. The primary function of domain II is to help specify the electrophilic substrate preference of a particular isoenzyme. To this extent, the characterization of domain II as the xenobiotic substrate binding domain is apt.

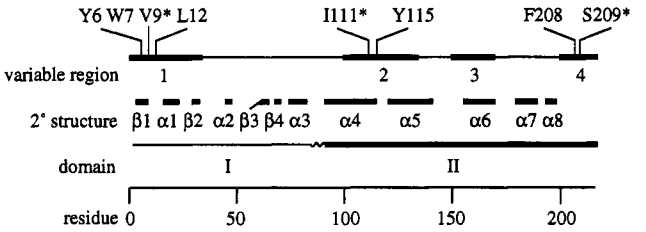

FIGURE 5: Schematic illustration of the relationship between the variable-sequence regions, the secondary structural elements, and the domain structure of isoenzyme 3-3. The residues that contact the dihydrophenanthrenyl moiety of the products are positioned at the top. Residues that differ between the type 3 and type 4 subunits are denoted with an asterisk.

What do the product complexes reveal about the stereoselectivity of the μ class isoenzymes? The type 3 subunit exhibits little stereoselectivity toward phenanthrene 9,10-oxide,

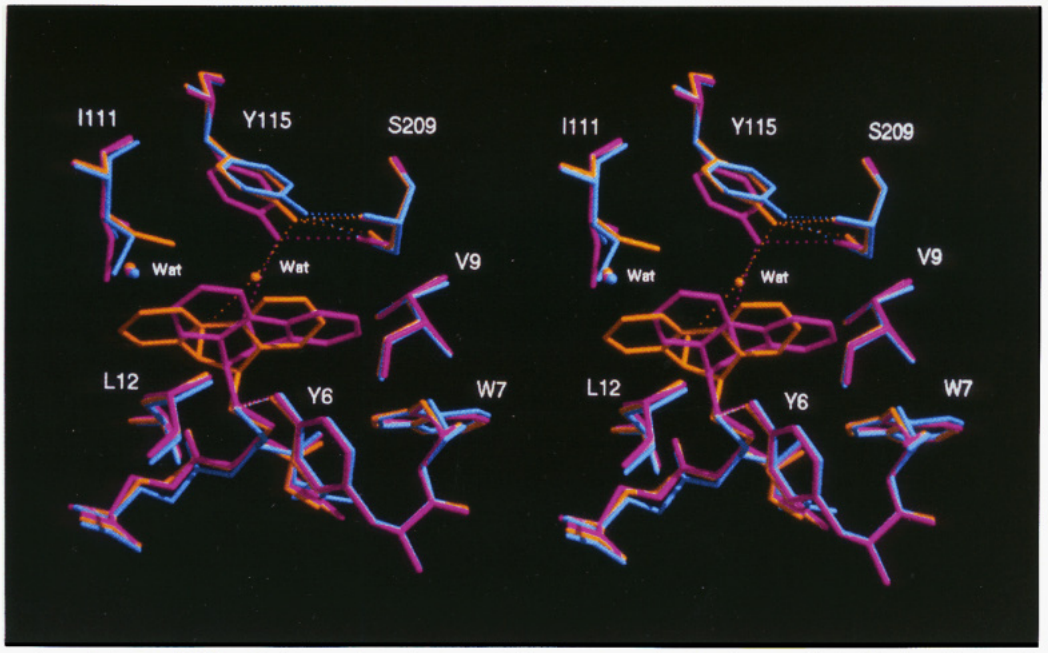

FIGURE 6: Stereoview of the RASTER 3D (Bacon & Anderson, 1988) representation for the xenobiotic binding site in subunit A of μ class glutathione *S*-transferase 3-3 complexed with glutathione (blue; Ji *et al.*, 1992), with (9*R*,10*R*)-9-(*S*-glutathionyl)-10-hydroxy-9,10-dihydrophenanthrene (yellow), and with (9*S*,10*S*)-9-(*S*-glutathionyl)-10-hydroxy-9,10-dihydrophenanthrene (pink). The conserved water molecule bound in the hydrophobic pocket and within van der Waals distance of the 9,10-dihydrophenanthrenyl group is included.

while the type 4 subunit favors catalyzing the attack of GSH at the oxirane carbon of *R* absolute configuration to give (9*S*,10*S*)-**2**. The latter fact is made more interesting since it is not easily reconciled with the structures of the product complexes of the type 3 subunit. The three residues proximal to the xenobiotic substrate binding site that differ between the type 3 and 4 subunits (e.g., V9I, I111A, and S209A) are obvious candidates for close scrutiny with respect to the stereoselectivity of the isoenzymes. Overall, these three mutations are expected to make the substrate binding site of the type 4 subunit a bit larger and less congested than that of the type 3 subunit, since two of the three mutations result in smaller side chains. However, it appears from Figures 3 and 6 that the one side chain that increases in size (V9I) in the type 4 subunit would increase steric crowding, particularly toward the favored product, (9*S*,10*S*)-**2**, of isoenzyme 4-4. Previous modeling (Zhang *et al.*, 1992) of the position of the mutant I9 side chain in the active site shows that the *S* arm extends about 1 Å further into the active-site cavity than does the *pro*-*S*-methyl group of V9. This extension would create an unfavorable van der Waals contact for (9*S*,10*S*)-**2** as bound in the active site of isoenzyme 3-3 and, by implication, in the active site of isoenzyme 4-4 as well. This is contrary to the simple expectation that the favored product would be more easily accommodated since it is derived from the more favored transition state. Hence, either the active site of isoenzyme 3-3 is not a suitable model from which to draw conclusions about the behavior of the type 4 subunit, or the structures of the products are poor models for the transition states of the reaction.

Are the products good structural analogues of the transition states for oxirane ring opening reactions? Drawing specific conclusions about the stereoselectivity of isoenzymes 3-3 and 4-4 from the structures of product complexes presupposes that the products resemble the transition states leading to their formation. The addition of sulfur nucleophiles to arene oxides occurs with β_{nuc} values ≤ 0.2, suggesting that these reactions proceed through an early, reactant-like transition state (Bruice *et al.*, 1976). The two product structures are probably not accurate representations of the diastereomeric transition states and cannot be used to quantitatively predict the distribution of products in either isoenzyme. Nevertheless, the structural results are valuable for pinpointing specific residues that are likely to influence catalysis and provide useful starting points for molecular dynamics simulations. Preliminary results[2] suggest that the single mutants V9I and I111A of isoenzyme 3-3 have stereoselectivities and catalytic efficiencies toward phenanthrene 9,10-oxide and 4-phenyl-3-buten-2-one that begin to mimic those of the type 4 subunit.

Role of Y115 in Catalysis. The proximity of the hydroxyl group of Y115 to the hydroxyl group of the product suggests that this side chain may be appropriately positioned to provide electrophilic assistance in the addition of GSH to epoxides. In fact, the Y115F mutant of isoenzyme 3-3 is about 100-fold less efficient than the native enzyme at catalyzing the addition of GSH to **1** (Johnson *et al.*, 1993). The similar decrease in efficiency of the mutant toward 4-phenyl-3-buten-2-one (**3**) (Table 3) suggests an equivalent involvement of the hydroxyl group of Y115 in Michael additions. Both of these reactions would benefit from electrophilic assistance in the stabilization of oxyanions, as illustrated in Figure 7. The extent of transition-state stabilization affected by the hydroxyl group of Y115 is small, on the order of 2–3 kcal/mol. However, it is enough to substantially affect the substrate specificity of a given isoenzyme. In this regard, it is interesting to note that GSH transferases such as the α class isoenzymes (Mannervik *et al.*, 1985) or the squid enzyme (Tomarev *et al.*, 1993), which do not have a tyrosine residue at the equivalent position of Y115, are not particularly good for catalyzing epoxide ring openings or Michael additions.[3] The structural and functional evidence suggests that Y115 acts as a general-acid catalytic group.

Although the structure of E·(9*S*,10*S*)-**2** suggests that Y115 may provide electrophilic assistance through a direct hydrogen

[2] S. Shan and R. N. Armstrong, unpublished results.

[3] W. W. Johnson, S. I. Tomarev, and R. N. Armstrong, unpublished results.

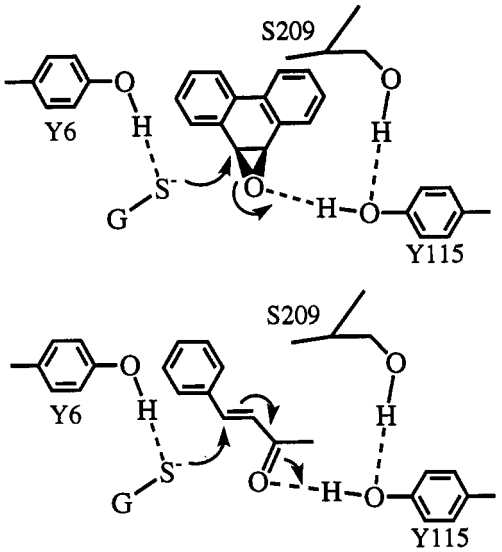

FIGURE 7: Proposal for electrophilic assistance by the hydroxyl group of Y115 in Michael additions and oxirane ring openings. The two tyrosine residues represent a classical push–pull catalytic ensemble in these reactions.

bond to the oxirane oxygen in the transition state, the alternative, that the assistance is transmitted by an intervening water molecule, cannot be excluded. This possibility is supported by the observation of a water molecule in the structure of the E·(9*R*,10*R*)-**2** complex, which bridges the hydroxyl groups of the product and Y115. However, there is no water molecule at this position in the structure of the E·GSH complex (Ji *et al.*, 1992).

The hydroxyl group of Y115 is also involved in the product release step of the enzymatic reaction. When product release is the rate-limiting step in turnover as it is with 1-chloro-2,4-dinitrobenzene (Johnson *et al.*, 1993), the Y115F mutant has a higher turnover number than the native enzyme. It is possible that the hydrogen-bonding interactions between the hydroxyl groups of Y115 and S209 (Figures 6 and 7), which help tie together the α4-helix and the C-terminal tail of the protein, decrease the segmental motion of the protein and inhibit product release. A similar increase in the rates of dissociation of (9*R*,10*R*)-**2** and (9*S*,10*S*)-**2** from the Y115F mutant is observed, though product release is not the rate-limiting step in the addition of GSH to **1**. It is not possible to define the exact nature of the hydrogen-bonding interaction between S209 and the hydroxyl group of Y115 from the crystal structure. In contrast to Figure 7, it is conceivable that the hydroxyl group of Y115 acts as a hydrogen-bond donor to the hydroxyl group of S209. However, this configuration would not permit Y115 to provide electrophilic assistance in the reactions above, as appears to be the case.

Further evidence that interactions between the μ loop, the α4-helix, and the C-terminal tail affect the rate of dissociation of products can be seen in the behavior of (9*R*,10*R*)-**2** and (9*S*,10*S*)-**2**. At first glance it might be expected that (9*S*,10*S*)-**2** would have a lower dissociation constant and a smaller rate constant for dissociation than the other diastereomer since it benefits from a direct hydrogen bond between the 10-hydroxyl group and Y115. Qualitatively, this does appear to be true in the crystal. However, just the opposite is true in solution. The dissociation constant for the (9*R*,10*R*) diastereomer (0.19 μM) is about 4-fold lower than that for (9*S*,10*S*)-**2** (0.85 μM), as measured by product inhibition (Chen *et al.*, 1986). Furthermore, the rate constant for dissociation of (9*R*,10*R*)-**2** (2.6 s^{-1}) is slightly lower than that for (9*S*,10*S*)-**2** (4.4 s^{-1}), as measured by stopped-flow studies (Johnson *et al.*, 1993). Thus, the dissociation behavior of the products in solution appears to correlate with the more extensive hydrogen-bonding network (Table 4) between the three structural elements that help define the approach to the active site. Unfortunately, the extent to which the observed hydrogen-bonding network is dependent on crystal packing effects is not clear. However, the different exchange behavior of the two diastereomers in the crystal and solution obviously suggests that crystal lattice effects have a significant influence on the dynamics in the crystal. Additional, carefully chosen site-specific mutants may help clarify the interactions important to the dynamics of product release in solution.

Conclusions. The three-dimensional structures of isoenzyme 3-3 of GSH transferase complexed with the products of addition of GSH to phenanthrene 9,10-oxide reveal the identities of several residues in the xenobiotic binding domain of the enzyme that influence catalysis. All of the residues involved in the xenobiotic substrate binding site are located in variable-sequence regions of the enzyme, an observation that suggests that the variable regions have evolved to increase the catalytic diversity of this group of proteins. The hydroxyl group of Y115 located in domain II is an electrophilic participant in catalysis and, at least in part, explains the higher catalytic efficiency of the μ class isoenzymes toward epoxide and α,β-unsaturated ketones. Domain II of the μ class GSH transferases plays a significant role in defining the substrate specificity of the enzyme.

SUPPLEMENTARY MATERIAL AVAILABLE

One table showing the data collection statistics by resolution shells for both data sets (2 pages). Ordering information is given on any current masthead page.

REFERENCES

Abramovitz, M., & Listowsky, I. (1987) *J. Biol. Chem. 262*, 7770–7773.

Armstrong, R. N. (1991) *Chem. Res. Toxicol. 4*, 131–140.

Armstrong, R. N. (1994) *Adv. Enzymol. Relat. Areas Mol. Biol. 69* (in press).

Bacon, D., & Anderson, W. A. (1988) *J. Mol. Graphics 6*, 219–220.

Bernstein, F. C., Koetzle, T. F., Williams, G. J. B., Meyer, E. F., Jr., Brice, M. D., Rogers, J. R., Kennard, O., Shimanouchi, T., & Tasumi, M. (1977) *J. Mol. Biol. 112*, 535–547.

Boehlert, C. C., & Armstrong, R. N. (1984) *Biochem. Biophys. Res. Commun. 121*, 980–986.

Bruice, P. Y., Bruice, T. C., Yagi, H., & Jerina, D. M. (1976) *J. Am. Chem. Soc. 98*, 2973–2981.

Chen, W.-J., deSmidt, P. C., & Armstrong, R. N. (1986) *Biochem. Biophys. Res. Commun. 141*, 892–897.

Cobb, D., Boehlert, C., Lewis, D., & Armstrong, R. N. (1983a) *Biochemistry 22*, 805–812.

Cobb, D. I., Lewis, D. A., & Armstrong, R. N. (1983b) *J. Org. Chem. 48*, 4139–4141.

Chung, H., Harvey, R. G., Armstrong, R. N., & Jarabak, J. (1987) *J. Biol. Chem. 262*, 12448–12451.

Furey, W. (1990) *Abstracts of the American Crystallographic Association Fortieth Anniversary Meeting*, New Orleans, LA, PA33, American Crystallographic Association, Buffalo, NY.

Furey, W., Wang, B. C., & Sax, M. (1982) *J. Appl. Crystallogr. 15*, 160–166.

Hendrickson, W. (1985a) *Methods Enzymol. 115*, 252–270.

Hendrickson, W. (1985b) *Crystallographic Computing 3: Data Collection, Structure Determination, Proteins, and Databases* (Sheldrick, G., Kruger, C., & Goddard, R., Eds.) pp 306–311, Clarendon Press, Oxford, U.K.

Hendrickson, W., & Konnert, J. (1980a) *Computing in Crystallography* (Diamond, R., Ramaseshan, S., & Venkatesan, K., Eds.) pp 1301–1323, Indian Academy of Sciences, Bangalore, India.

Hendrickson, W., & Konnert, J. (1980b) *Biomolecular Structure, Function, Conformation and Evolution* (Srinivasan, R., Ed.)Vol. 1, pp 43–57, Pergamon, Oxford, U.K.

Howard, A. J., Gilliland, G. L., Finzel, B. C., Poulos, T. L., Ohlendorf, D. H., & Salemme, F. R. (1987) *J. Appl. Crystallogr. 20*, 383–387.

James, M. N. G., & Sielecki, A. R. (1983) *J. Mol. Biol. 163*, 299–361.

Ji, X., Zhang, P., Armstrong, R. N., & Gilliland, G. L. (1992) *Biochemistry 31*, 10169–10184.

Johnson, W. W., Liu, S., Ji, X., Gilliland, G. L., & Armstrong, R. N. (1993) *J. Biol. Chem. 268*, 11508–11511.

Jones, T. A. (1978) *J. Appl. Crystallogr. 11*, 268–272.

Mannervik, B., Alin, P., Guthenberg, C., Jensson, H., Tahir, M. K., Warholm, M., & Jornvall, H. (1985) *Proc. Natl. Acad. Sci. U.S.A. 82*, 7202–7206.

Reinemer, P., Dirr, H. W., Ladenstein, R., Schaffer, J., Gallay, O., & Huber, R. (1991) *EMBO J. 10*, 1997–2005.

Rushmore, T. H., & Pickett, C. B. (1993) *J. Biol. Chem. 268*, 11475–11478.

Sesay, M. A., Ammon, H. L., & Armstrong, R. N. (1987) *J. Mol. Biol. 197*, 377–378.

Siegel, F., Neal, T. L., Johnson, J. A., Bertics, P. J., & Wright, L. S. (1990) in *Glutathione S-Transferases and Drug Resistance* (Hayes, J. D., Pickett, C. B., & Mantle, T. J., Eds.) pp 47–56, Taylor & Francis, London.

Sinning, I., Kleywegt, G. J., Cowan, S. W., Reinemer, P., Dirr, H. W., Huber, R., Gilliland, G. L., Armstrong, R. N., Ji, X., Board, P. G., Olin, B., Mannervik, B., & Jones, T. A. (1993) *J. Mol. Biol. 232*, 192–212.

Tomarev, S. I., Zinovieva, R. D., Gou, K., & Piatigorsky, J. (1993) *J. Biol. Chem. 268*, 4534–4542.

Zhang, P., & Armstrong, R. N. (1990) *Biopolymers 29*, 159–169.

Zhang, P., Graminski, G. F., & Armstrong, R. N. (1991) *J. Biol. Chem. 266*, 19475–19479.

Zhang, P., Liu, S., Shan, S., Ji, X., Gilliland, G. L., & Armstrong, R. N. (1992) *Biochemistry 31*, 10185–10193.